AIChE WILEY InterScience DISCOVER SOMETHING GREAT

Structure of Operating Domains of Loop Reactors

Olga Nekhamkina and Moshe Sheintuch
Dept. of Chemical Engineering, Technion-Israel Institute of Technology, Haifa 32 000, Israel

DOI 10.1002/aic.11462
Published online March 17, 2008 in Wiley InterScience (www.interscience.wiley.com).

A loop reactor (LR), composed as an N-unit loop with step-wise shifted inlet and outlet ports, is one of suggested technological solutions for low-concentration volatile organic compounds (VOC) combustion. Such a scheme ensures a sufficiently high temperature with autothermal behavior and nearly uniform catalytic utilization. The main drawback of the LR is a very narrow window of switching velocities that sustain a stable "frozen" solution that exists if the switching and the pulse velocity are synchronized. In the present work we show the existence of many "finger"-like domains of complex frequency-locked solutions that allow to significantly extend the operation domain, rendering the LR scheme more attractive for practical implementation. A brief comparison with the other heat recuperation technologies (reverse flow and circular loop reactors) is presented.
 AIChE J, 54: 1292–1302, 2008
Keywords: reactor analysis, simulation process, packed bed, bifurcations

Introduction

The loop reactor in the form composed of several units, with feed switching between them (Figure 1a), is one of suggested technological solutions for low-concentration VOC combustion. Other conceptual solutions that combine a packed bed with enthalpy recuperation include the reverse-flow reactor,[1–3] the counter-current or the internal-recycle reactor (CCR)[4–6] and the reactor with external recycle and external heat exchanger.[5,7,8] Another form of a circulating loop-reactor (CLR, Figure 1b), in which the entrance region is heated via a heat-exchanger by the exit stream, was suggested by Lauschke and Gilles[9] and tested experimentally.[10]

The loop or ring reactor has been proposed by Matros[11] and was simulated for a case of two units by Haynes and Caram[12] or for three units by Barresi and coworkers[13–19] for certain applications like VOC abatement and exothermic reversible reactions. This concept is based on a temperature pulse (hot spot) rotating around the system with a certain velocity (V_{fr}) subject to external forcing defined by the switching velocity ($V_{sw} = \Delta L/\tau_{sw}$, i.e. unit length divided by switching time). Stable solutions of the LR exist with a certain matching of both velocities (or related frequencies). In our previous works (Sheintuch and Nekhamkina[20,21]) we derived the asymptotic LR model, showing the existence of a slow switching solution with $V_{fr} = V_{sw}$, which is "frozen" in rotating coordinates. It was shown that the pulse velocity can be varied within a certain range approximately bounded by the "ideal" front velocity in an infinitely long system (V_{fr}^{id}) and the heat front velocity ($V_{th} = 1/Le$). These limiting values define the low switching velocity domain of simple 1:1 (the ratio V_{fr}:V_{sw}) patterns: $V_{sw}^{min} < V_{sw} < V_{sw}^{max}$. This domain is very narrow[12,15,20] and appears to be the main drawback of the LR operating in a "frozen" mode. However, another asymptote, that of a fast switching solution in which V_{sw} significantly exceeds V_{fr}, was also shown to exist.[20] Existence of the fast switching operation domain ($V_{sw} > V_{fr}$) for the three-unit LR was reported in series of numerical studies.[16–18] The first experimental implementations of the LR were recently reported for an almost isothermal process (selective catalytic reduction, NH_3 + NO, Fissore et al.[19]) and for the VOC combustion concept in the slow-switching domain (ethylene oxidation, Madai and Sheintuch[22]).

In the present study we analyze the LR behavior in the domain between the two asymptotes and show that in the parametric plane (p, V_{sw}), where p is any of the parameters, complex (1:n) type solutions exist within certain subdomains of

Correspondence concerning this article should be addressed to O. Nekhamkina at aermwon@tx.technion.ac.il and M. Sheintuch at cermsll@technion.ac.il.

"finger"-like form (Arnold "tongues"). The width of each subdomain in length of V_{sw} expands with increasing feed concentration. "Frozen" solutions exist only in one of the fingers. The existence of non-"frozen" solutions allows to extend significantly the operation condition domain rendering the LR scheme more attractive for practical implementation. The exact mapping is important since these subdomains are separated by domains of extinguished solutions. Thus, the significance of this mapping goes beyond the academic interest in the solution structure of spatio-temporal forcing of a reactor with periodic boundary conditions. The chaotic solutions and the bifurcation scenarios leading to chaos were studied numerically for a three-unit LR by Russo et al.[23] and Altimari et al.[24] A brief analysis of complex non-frozen solutions in a LR with different N was conducted in our previous works.[20,21] Note, that the complex dynamics emerging in this case is different from that simulated and observed for a packed bed in which an oscillatory reaction proceeds (Barto and Sheintuch,[25] Sheintuch and Nekhamkina,[26] Digilov et al.[27]).

Another object of this work is the comparison of the LR operating domain with those of RF and CLR units using their asymptotic solutions. In the early studies Haynes and Caram[12] and Fissore and Barresi[15] numerically compared the LR operating within the slow-switching domain with the RFR to conclude that the LR advantages include significant reduction of the washout effect, the autothermal behavior and nearly uniform catalyst utilization. The circular loop reactor (CLR) produces a gradually varying rotating pulse solution and in its limiting case it can be formally considered as a limiting case of a loop reactor network with $N = 1$ and $V_{sw} \to 0$. Thus, the front velocity (V_{fr}), as well as the maximal temperature (T_m) behind the front are essential parameters that define the reactor behavior for both the LR and for the CLR. In catalytic systems the moving pulse temperature can be increased significantly by pushing the front. For a case of a single irreversible reaction in an ideal front (i.e. in an infinitely long system) T_m and V_{fr}^{id} admits the following relations (Wicke and Vortmeyer[28]):

$$\Delta T_m = T_m - T_0 = \Delta T_{ad}\frac{v - V_{fr}^{id}}{v - Le V_{fr}^{id}}, \quad V_{fr}^{id} = v\frac{\Delta T_{ad} - \Delta T_m}{\Delta T_{ad} - Le\Delta T_m}, \tag{1}$$

Obviously, the front velocity cannot exceed the thermal front velocity $V_{th} = v/Le$ which corresponds to an infinitely large temperature rise in the ideal front. In a finite length once-through reactor the pulse will eventually leave the system and the extinguished state will prevail. Thus, some form of matched boundary conditions or external periodic forcing are required to sustain the periodic motion, and its analysis is the aim of this work.

The structure of this work is the following: in the next section we review the asymptotic and the finite unit LR model formulated in our previous study.[20] In the third section the approximate relations for the maximal temperature rise in reactors of various types are presented. The fourth section portrays the intricate "finger"-like structure of the operating domain of the LR. In the last section a brief comparison of the LR with the other heat recuperation reactor schemes is discussed.

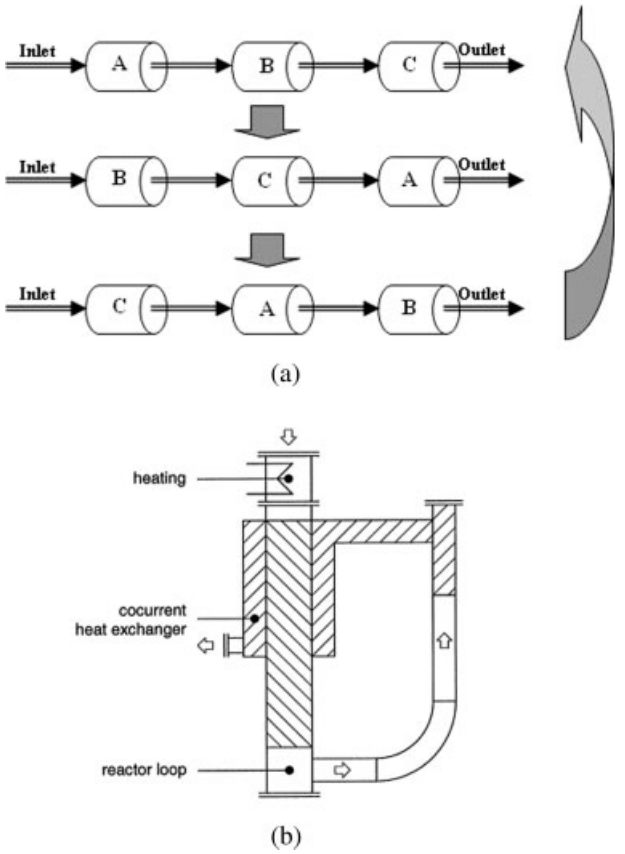

Figure 1. Schemes of a three-unit loop reactor (LR, a) and a circular loop reactor (CLR, b after Ref. 9).

Reactor Model

We limit our study to a generic first-order activated and exothermic reaction, reacting at a rate of $r = A\exp(-E/RT)C$. The dispersivity (D_f), conductivity (k_e) and thermodynamic parameters [ρ, c_p, $(-\Delta H)$] are assumed to be constant. Under these assumptions the enthalpy and mass balances may be written in the following dimensionless form:

$$Le\frac{\partial y}{\partial \tau} + v\frac{\partial y}{\partial \xi} - \frac{1}{Pe_y}\frac{\partial^2 y}{\partial \xi^2} = BDa(1-x)\exp\left(\frac{\gamma y}{\gamma + y}\right) = B(1-x)f(y) \tag{2}$$

$$\frac{\partial x}{\partial \tau} + v\frac{\partial x}{\partial \xi} - \frac{1}{Pe_x}\frac{\partial^2 x}{\partial \xi^2} = Da(1-x)\exp\left(\frac{\gamma y}{\gamma + y}\right) = (1-x)f(y) \tag{3}$$

with appropriate initial and boundary conditions. In the case of a once-through operation the Danckwerts' BC are typically employed:

$$\begin{aligned} &\xi = \xi_{in}, \quad \frac{1}{Pe_y}\frac{\partial y}{\partial \xi} = v(y - y^{in}), \quad \frac{1}{Pe_x}\frac{\partial x}{\partial \xi} = v(x - x^{in}), \\ &\xi = \xi_{out}, \quad \frac{\partial y}{\partial \xi} = 0, \quad \frac{\partial x}{\partial \xi} = 0 \end{aligned} \tag{4}$$

Here conventional notation is used:

$$\xi = \frac{z}{z_0}, \quad \tau = \frac{tu_0}{z_0}, \quad y = \gamma\frac{T-T_0}{T_0}, \quad x = 1-\frac{C}{C_0}, \quad v = \frac{u}{u_0},$$
$$L = \frac{\tilde{L}}{z_0}, \quad \gamma = \frac{E}{RT_0}, \quad B = \frac{(-\Delta H)C_0\gamma}{(\rho C_p)_f T_0}, \quad Da = \frac{Az_0}{u_0}\exp(-\gamma),$$
$$Le = \frac{(\rho C_p)_e}{(\rho C_p)_f}, \quad Pe_y = \frac{(\rho C_p)_f z_0 u_0}{k_e}, \quad Pe_x = \frac{(\rho C_p)_f z_0 u_0}{D_f}.$$

Note, that we use arbitrary values (u_0, z_0) for the fluid velocity and the length scales in order to ensure that the corresponding dimensionless values (L, v) can be varied as independent parameters. Typically in our simulations, as well as in practical situations, $Le \gg 1$ and Pe_y, $Pe_x \gg 1$.

Multiport reactor

Consider a loop reactor of N identical units (each one of length $\Delta L = L/N$) with gradual switching of the inlet and outlet ports over each time interval σ. Such a reactor can be described by a continuous model Eqs. 2–4 if we ignore the end-effects of the intermediate sections and apply the boundary conditions at the feed inlet and outlet positions that vary in time as stepwise functions with a total period $\theta = N\sigma$:

$$\begin{aligned} &\xi_{in} = (m-1)\Delta L, \quad \xi_{out} = L-(m-1)\Delta L, \\ &\tau \in [(m-1)\sigma, m\sigma] + k\theta, \quad m = 1,\ldots,N;\ k = 0,1 \end{aligned} \tag{5}$$

Here m specifies the unit number and k is the cycle number.

Asymptotic continuous model (infinite port model)

In the limiting case of an infinite-port loop reactor ($N\to\infty$) the stepwise functions $\xi_{in}(\tau)$, $\xi_{out}(\tau)$ can be replaced by a continuous description of the feed positions[21]:

$$\zeta_{in} = \xi_{in}^0 - V_{sw}\tau, \quad \zeta_{out} = \xi_{out}^0 - V_{sw}\tau,$$

where the switching velocity (V_{sw}) is defined as $V_{sw} = \Delta L/\sigma$. In such a case it is convenient to transform the governing Eqs. 2 and 3 using a moving coordinate system ($\tau' = \tau$, $\zeta = \xi - V_{sw}\tau$) with fixed positions of the inlet and outlet:

$$Le\frac{\partial y}{\partial \tau} + (v - LeV_{sw})\frac{\partial y}{\partial \zeta} - \frac{1}{Pe_y}\frac{\partial^2 y}{\partial \zeta^2} = B(1-x)f(y) \tag{6}$$

$$\frac{\partial x}{\partial \tau} + (v - V_{sw})\frac{\partial x}{\partial \zeta} - \frac{1}{Pe_x}\frac{\partial^2 x}{\partial \zeta^2} = (1-x)f(y) \tag{7}$$

The mass balance Danckwerts' BC conditions (see Eq. 4) can still be applied in this case. For the energy balance equation, in the case of slow switching, the appropriate boundary conditions were shown[20] to be:

$$\frac{1}{Pe_y}\left[\left(\frac{\partial y}{\partial \zeta}\right)_{in} - \left(\frac{\partial y}{\partial \zeta}\right)_{out}\right] = v(y - y^{in}), \quad y_{in} = y_{out} \tag{8}$$

The first of conditions (8) was derived as a simple combination of the Danckwerts' BC, while the second condition enable the formation of a pulse solution and was verified in our previous work: we have numerically shown[20] that the solution of the multiport reactor Eqs. 2–4 converges to the asymptotic model Eqs. 6–8 as $N\to\infty$.

Note, that for the CLR model (see Appendix, Figure 1b), which combines a heat exchanger between the inlet and outlet streams, the first of conditions (8) can be applied as well, while the second condition can be implemented in the limiting case of an infinitesimal heat exchange region (Δ) and an infinite heat exchange coefficient (α). Thus, the limiting CLR model ($\alpha\to\infty$, $\Delta\to 0$) coincides with the asymptotic LR model with $V_{sw} = 0$.

Front Characteristics

We consider here analytical approximations for the maximal temperature (T_m) and the front velocity (V_{fr}) that can be reached in the various reactors. These are used to compare the efficiency of the various reactor schemes. While high T_m by itself is not the objective for low-concentration VOC combustion, but rather a wide domain of state operation (i.e. the extinction point), such domains cannot be predicted analytically.

An approximate relation for an "ideal" front in an infinitely long system was derived by Kiselev[29] using the narrow reaction zone assumption proposed by Frank-Kamenetski[30]:

$$\frac{BPe_y(v - V_{fr}^{id})^2}{(1+y_m/\gamma)^2 Da\,\exp[y_m/(1+y_m/\gamma)]} = 1 \tag{9}$$

The dimensionless front velocity V_{fr}^{id} and the maximal temperature y_m are related (see Eq. 1) by:

$$V_{fr}^{id} = v(B - y_m)/(B - Ley_m) \tag{10}$$

within the domain

$$-\infty < V_{fr}^{id} < V_{th} = 1/Le, \quad B/Le < y_m < \infty \tag{11}$$

Substituting Eq. 10 into Eq. 9 we obtain an equation with respect to a single unknown variable y_m:

$$\frac{BPe_y}{(1+y_m/\gamma)^2 Da\,\exp[y_m/(1+y_m/\gamma)]}\left[\frac{(Le-1)v}{Le - B/y_m}\right]^2 = 1 \tag{12}$$

For a sufficiently long circular loop reactor T_m can be estimated as that corresponding to an infinitely long system.

For a fast-switching reverse flow reactor with a stationary front position ("sliding" regime) a similar relation was derived by Matros[11]:

$$\frac{BPe_y}{(1+y_m/\gamma)^2 Da\,\exp[y_m/(1+y_m/\gamma)]}\left[\frac{(Le-1)v}{Le - B/y_m}\right]^2 = 2 \tag{13}$$

For a loop reactor, within the low-switching operation domain, the switching velocity V_{sw} can be varied in a certain interval ($V_{sw}^{mn} < V_{sw} < V_{sw}^{mx}$) leading to formation of a quasi-frozen rotating pattern. In such a case the front velocity is prescribed (equal to V_{sw}) and we recently derived[31] two

approximate relations between the maximal temperature (y_m) and V_{sw}:

(i) If a complete conversion is achieved at the front ($x_m = 1$), than:

$$\frac{BPe_y(v - V_{sw})^2}{(1 + y_m/\gamma)^2 Da \exp[y_m/(1 + y_m/\gamma)]} = 1 + \beta(y_m, V_{sw}) \quad (14)$$

where $\beta(y_m, V_{sw})$ is a correction due to non-homogeneous BC. Equation 14 is reduced to Eq. 9 for the "ideal" front propagation in the infinitely long system (i.e. $\beta = 0$) with V_{fr}^{id} replaced by V_{sw}.

(ii) For the incomplete conversion case ($x_m \neq 1$) we obtained a system with respect to two unknown variables y_m and x_m:

$$\frac{BPe_y(v - V_{sw})^2}{(1 + y_m/\gamma)^2 Da \exp[y_m/(1 + y_m/\gamma)]} = \frac{1}{x_m + \omega(y_m, x_m, V_{sw})} \quad (15)$$

$$(v - LeV_{sw})[y_m - y(0)] + 2B(v - V_{sw})x_m = \frac{B(v - V_{sw})(1 + y_m/\gamma)^2 x_m^3}{(x_m + \omega)(1 - x_m)[y_m - y(0)]} \quad (16)$$

where ω (y_m, x_m, V_{sw}) is a correction due to non-homogeneous BC and incomplete conversion.

Windows of Operation of Loop Reactors

We portray now the domains of existence of ignited solutions in the B vs. V_{sw}/V_{th} plane. These domains form "fingers" of frozen and non-frozen solutions. Previous simulations[20,21] have described one-parametric bifurcation diagrams (as a function of V_{sw}) and revealed one or two such domains; these are extended here to two-dimension maps that show many such domains. The system also attains an extinguished solution for the whole domain, while ignited patterns can be sustained with a proper choice of initial conditions (IC). The parameters used are those employed by Eigenberger and Nieken[2] and used later by Haynes and Caram[12] and in our previous studies.[20,21]

We start with analysis of the asymptotic continuous model, which successfully approximates the domain of operation of quasi-"frozen" solutions in the infinite-unit model,[20] and follow by analysis of the discrete-port model.

Continuous model

Bifurcation Diagram. The domain of "frozen" patterns (FP) forms a cusp-like structure that expands with increasing feed concentration or adiabatic temperature rise (B) (Figure 2a, with constant v) and shrinks with increasing convective velocity v (Figures 2b, c with constant B). The lower-switching boundary V_{sw}^{mn} was analyzed elsewhere[31] to show it can be approximated from Eq. 14, while the upper-switching boundary (V_{sw}^{mx}) can be predicted using set Eqs. 15 and 16. The lower boundary (V_{sw}^{mn}) decreases with increasing B and intersects the ordinate at $B = B_{cr}$ ($\approx$13.8 B_0 for $v = 1$, Figure 2a), i.e. beyond B_{cr} patterns can emerge in a loop reactor without any forced switching ($V_{sw} = 0$) and such a reactor can be constructed as a single section with properly matched inlet and outlet. With increasing convective velocity (v) the boundaries of the FP domain, defined via a normalized switching velocity V_{sw}/V_{th}, gradually approach each other (Figures 2b, c).

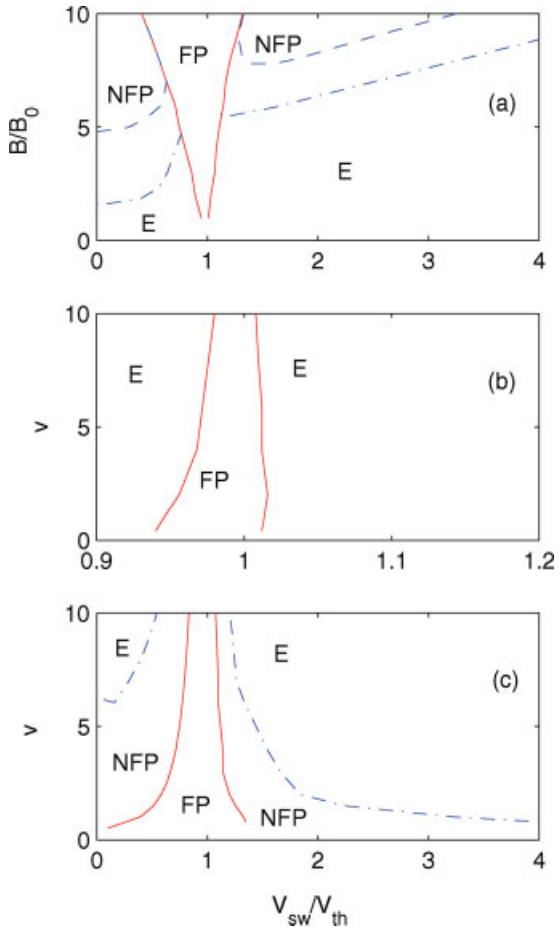

Figure 2. Bifurcation map of the asymptotic loop reactor model in the (B/B_0, V_{sw}/V_{th}) plane (a, $v = 1$) and in the (v, V_{sw}/V_{th}) plane (b, $B = B_0$; c, $B = 10B_0$) showing domains of frozen (FP, solid lines) by non-frozen (NFP, dashed with $L = 1$ and dashed-dotted with $L = 8$) and extinguished (E) solutions.

Other parameters are those, used by Eigenberger and Nieken[4]: $C_0 = 1.21 \times 10^{-4}$ kmol/m^3, $E/R = 8000$ K, $(-\Delta H) = 206{,}000$ kJ/kmol, $A = 29{,}732$ s^{-1}, $u_0 = 1$ m/s, $z_0 = 1$ m, $T_{in} = 293$ K, $D = 5 \times 10^{-3}$ m^2/s, $k_e = 2.06 \times 10^{-3}$ kW/m/K, $(\rho C_p)_g = 0.5$ kJ/m^{3}K; $(\rho C_p)_e = 400$ kJ/m^{3}K, which result in $\Delta T_{ad}^0 = C_0(-\Delta H)/(\rho C_p)_g = 50$ K, $Pe_x = 200$; $Pe_y = 194$; $Le = 800$ and $B_0 = 0.523$ (calculated with $T_0 = 873$ K used as an initial condition for most simulations). [Color figure can be viewed in the online issue, which is available at www.interscience.wiley.com.]

Nonfrozen rotating patterns (NFP) exist in two domains adjacent to the FP domain on its two sides: The domain on the left (NFP$_1$, $V_{sw} < V_{sw}^{mn}$) extends up to $V_{sw} = 0$ for moderate v with large B (Figure 2c) and shifts toward larger V_{sw} with increasing v. The domain on the right of the FP (NFP$_2$, $V_{sw} > V_{sw}^{mx}$), as well as the others detected domains, shrinks with increasing v. Both NFP domains are strongly dependent on the reactor length (Figures 2a, c).

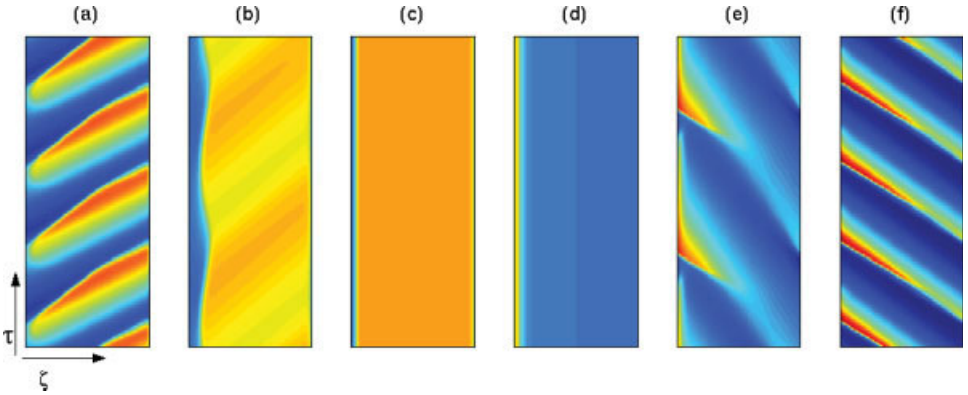

Figure 3. Typical temperature patterns of the asymptotic LR model in a coordinate system (ζ, τ) moving at velocity V_{sw} and theirs transformation with varying the switching velocity V_{sw}.

Shown are non-frozen rotating patterns in the left NFP_1 domain (V_{sw}/V_{th} = 0, a; 0.4, b), frozen patterns (V_{sw}/V_{th} = 0.48, c; 1.25, d) and non-frozen rotating patterns in the NFP_2 domain (V_{sw}/V_{th} = 1.36, e; 2.4, f), $B = 10B_0$, $v = 1$, $L = 1$. Other parameters as in Figure 2. [Color figure can be viewed in the online issue, which is available at www.interscience.wiley.com.]

A typical temperature pattern transformation, upon varying the switching velocity within both the NFP and the FP domains, is illustrated by Figure 3 showing the temperature patterns in the (ζ, τ) plane (i.e. in a coordinate system moving with the switching velocity V_{sw}). The solution presents right- and left-propagating waves for the left- and right NFP domains (Figures 3a, b, e, f), respectively, and stationary solutions within the FP domain (Figures 3c, d). Note, that in a laboratory coordinate system the rotating velocity is positive within the whole oscillatory domain (i.e. the ignited pulse propagates downstream).

Typical spatial temperature and conversion profiles which can be sustained without an external forcing ($V_{sw} = 0$) within the NFP_1 domain are shown in Figures 4a, b (in a laboratory coordinate). During a cycle a hot spot emerges at a certain position and propagates downstream with gradually increasing maximal temperature. Before leaving the reactor the moving hot spot heats up the cold inlet section and for a certain part of the cycle the reactor is practically extinguished. Recall that this represents a limit of the CLR. Simulations of the CLR with heat exchange sections of a finite length ($\Delta = 0.15$) under the same other conditions are shown in Figure 4c. Comparing these results with the temperature profiles of the LR (Figure 4a) one can see the similarity between both models, while the quantitative differences (the length of the ignited pulses, compare 5th profiles in Figures 4a, c) is obviously related with the existence of the finite length heat exchange sections in the CLR.

With increasing switching velocity V_{sw} the ignited spot in the LR is gradually shifted downstream and expands so that the separated pulses are fused yielding a continuous ignited domain (Figure 3b), and finally, above V_{sw}^{mn}, a "frozen" rotating pattern.

Within the FP domain, as was shown in previous studies,[20,21] the system exhibits a "frozen" pulse rotating with a constant (switching) velocity (Figures 3c, d). Within this domain increasing the switching velocity shifts the ignited front position (ζ_m) upstream when $V_{sw} < V_{th}$, while the opposite tendency takes place when $V_{sw} > V_{th}$.

Within the right-hand NFP_2 domain, just beyond the bifurcation point (V_{sw}^{mx}), the sustained pattern is composed of a continuous slightly varying pulse (near the reactor inlet) which periodically "fires" short pulses downstream (in a rotating coordinate system the pulses propagate in the opposite direction, Figures 3e, f). Typical temperature and conversion profiles are shown in Figure 4d, e. While most part of the reactor is cold, the exit conversion is sufficiently high due to the fast reaction within the ignited zone. Within the NFP_2 domain the pattern was found to admit a period-doubling bifurcation. Subsequent bifurcations can be also expected but such a study is beyond the scope of the present article.

Maximal Temperature Rise and Conversion. Up to three isolated branches exist as the switching velocity (V_{sw}) is varied: the maximal temperature (both in space and in time) and the average exit conversion are illustrated in Figures 5a–c. At low B values only the FP solution is sustained as an isolated branch, yielding good conversion, but over a relatively narrow domain, suggesting that some control is required. At higher B we can find either NFP_1 and/or NFP_2 isolated domains with high conversion for most part of subdomains. (The time-averaged exit conversion may become unsatisfactory only near the boundaries, Figure 5c). The maximal temperature slightly varies within both NFP subdomains. Within the FP domain the highest temperatures are achieved around $V_{sw} = V_{th}$.

The pulse propagation velocity obviously coincides with the switching velocity within the FP domain (Figure 5d). Within the NFP domains the period of oscillations is almost independent of V_{sw} yielding a practically constant velocity (averaged over a period of oscillation) close to the "ideal" front velocity $V_{fr}^{id} = V_{fr}^{id}(B)$, corresponding to an infinitely long system (Eqs. 9 and 10).

Effect of the System Length. The maximal temperature rise, conversion, as well as the boundaries of the "frozen" patterns, are only weakly dependent on the reactor length (L) in a sufficiently long system. The domains of NFP solutions extend with increasing L (Figures 2a, c). The "nonfrozen" solutions vary with time. The locus of spatial peaks within subdomain NFP_1 ascends downstream (Figure 4a) and extinction occurs if the lowest T_m falls below the ignition temperature. Within subdomain NFP_2 this locus ascends upstream (in

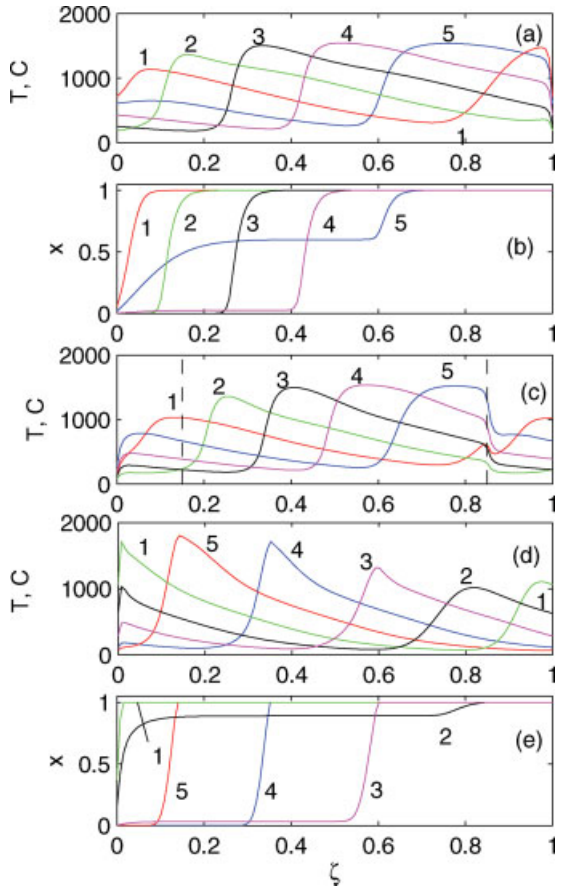

Figure 4. Typical sequence of asymptotic loop reactor temperature (a, d) and conversion (b, e) spatial profiles during one oscillation period within the NFP$_1$ domain (V_{sw} = 0, a, b) and within the NFP$_2$ domain (V_{sw}/V_{th} = 2.4, d, e).

Other parameters as in Figure 2. Plate (c) shows the temperature profiles in the circular loop reactor with a heat exchange section of length $\Delta = 0.15$ (its position is marked by dashed lines) and a dimensionless heat transfer coefficient $\alpha = 100$ simulated under the same other conditions. [Color figure can be viewed in the online issue, which is available at www.interscience.wiley.com.]

a rotating coordinate system, Figure 4d). Increasing L leads to increasing T_m reaching an asymptotic value close to the maximal temperature of an "ideal" front.

Discrete unit model

We extend now the analysis to the practical case of a small number of units (N). In this case the system can exhibit both simple solutions, rotating with a velocity equal to V_{sw}, and complex oscillations in the form of a continuous ignited pulse of a gradually varying form rotating with an average velocity V_{fr}, close to that of the "ideal" front velocity. Following the classification employed for the asymptotic model we refer to these solutions as quasi-frozen patterns (QFP) and quasi non-frozen patterns (QNFP). The non-frozen oscillations exhibit frequency locked solutions mainly of 1:n form defined by the ratio of the pulse rotation to the feed switching velocities.

Bifurcation Maps. Typical maps showing the "finger"-like domains of patterned states in the (B, V_{sw}/V_{th}) plane for systems with $N = 2$ and 4 are shown in Figure 6. The QFP subdomain and the "finger"-like QNFP domains are separated by gaps of extinguished states at low B. For large B the QNFP domains merge to yield a continuous domain with respect to varying V_{sw}.

The system exhibits a quasi-"frozen" pattern within the QFP domain rotating at $V_{fr}/V_{sw} = 1$. The QFP domain for a system with certain N is enclosed within the corresponding domain of the asymptotic model. The boundaries calculated for a two- and a four-unit system almost coincide and expand toward the limiting model with larger N.

Within the QNFP domains the system exhibits a spatially and temporally varying pulse (or several pulses) rotating with a velocity close to the "ideal" front velocity. For a set of parameters employed in this study we detected (with $N = 2$) large domains of 1:n solutions with odd $n = 3, 5, 7$ (we did not trace it further) and relatively small subdomains of even n, that exist only for large B. For such solutions the

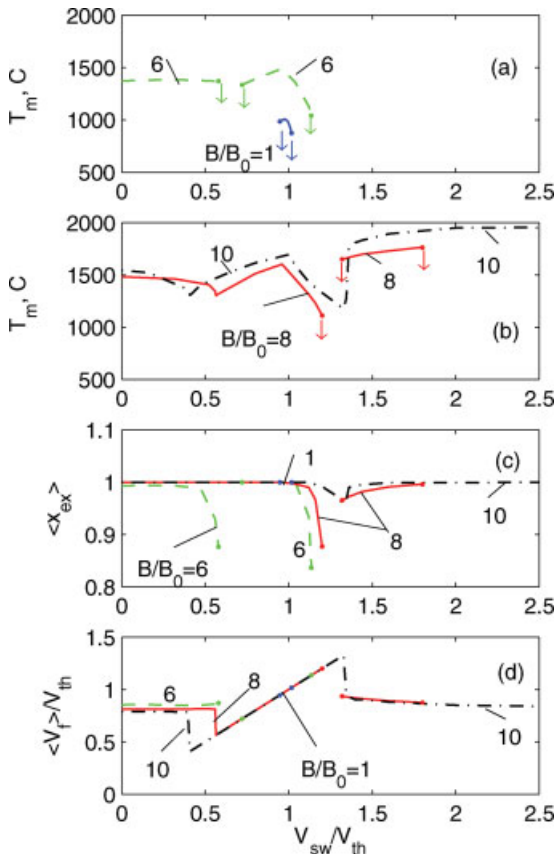

Figure 5. Typical bifurcation map of the asymptotic loop reactor model with varying switching velocity V_{sw} showing the maximal temperature T_m (a, b), the average exit conversion $\langle x_{ex}\rangle$ (c) and the average rotating pulse velocity $\langle V_{fr}\rangle$ (d).

Numbers mark B/B_0 values, downarrows in (a, b) and dots mark extinction points. $v = 1$, other parameters as in Figure 2. [Color figure can be viewed in the online issue, which is available at www.interscience.wiley.com.]

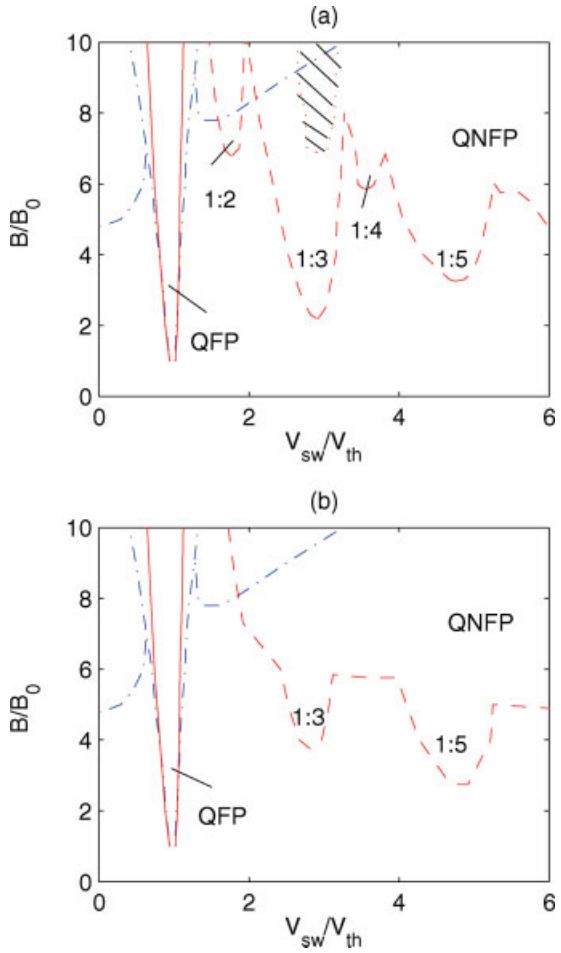

Figure 6. Typical structure of the finger-like domains of the two-unit (a) and four-unit (b) loop reactor model in the (B/B_0, V_{sw}/V_{th}) plane showing domains of quasi-frozen (QFP, solid lines) and quasi non-frozen (QNFP, dashed lines) solutions.

Dashed region shows subdomain of the $(1{:}3)_3$ solution. Dashed-dotted lines mark the boundaries of the FP and NFP domains of the asymptotic model. Numbers 1:n mark the type of the frequency locked solutions. [Color figure can be viewed in the online issue, which is available at www.interscience.wiley.com.]

total period of oscillations (P) coincides with the period of the pulse rotation (P_{fr}).

A typical 1:3 solution in a two-unit system is illustrated in Figures 7 and 8 by its spatio-temporal patterns in a laboratory coordinate system and by several equally intervaled spatial profiles. The sustained pattern repeats itself every N_n switches (six in this case) and admits the symmetry:

$$u(\xi,\tau) = u(\xi + L/M, \tau + P/M), \quad \xi \in [0, L/M],\ \tau \in [0, P/M] \tag{17}$$

where u is either of the state variables y and x, and $M = N = 2$. (Thus, Plates 1 and 4 of Figure 8 are shifted by a half domain and a half period and so on). During the 1st and the 3rd switching intervals (Figure 7) the feed enters unit 1 at the time when the ignited pulse is passing there, while during the second switching interval the feed enters through unit 2 which is behind the pulse and is completely extinguished. The temperature profiles vary along each switching (drastic changes take place when the front passes the currently switched inlet; interval 1, 4 of Figures 7 and 8). Conversion at the reactor exit is practically complete during the whole oscillation period as the flow stream always passes through the ignited pulse before exiting.

In addition to complex (1:n) solutions considered above we detected (at large B) multiperiodic patterns of $(1{:}n)_k$ type (i.e. k pulses coexist and move through the system, while the ratio of the pulse rotation and the switching velocities is 1 to n). A typical $(1{:}3)_3$ pattern exhibits three ignited pulses along the reactor (Figure 9) with an oscillation period equal to P_{fr}/k (i.e. coincides with the switching period for this particular case). Its subdomain in the parameter plane is shown in Figure 6 as a dashed region. Note that such patterns admit symmetry (17) with $M = N$, but are not spatially periodic at any fixed t. With increasing B the system may exhibit a rich plethora of patterns with complex $(m{:}n)_k$ frequency locking and extended subdomains of multiple solutions.

Effect of the Number of Units and the System Length. The boundary of the QNFP domain detected for a four-unit system is qualitatively similar to those of the two-unit LR (Figure 6) but is smoother. Note, that if symmetry (17) is preserved with $M = N$ for any pattern in a system of length L, we can expect that the same type of pattern can be sustained in a system with $N + 1$ units of length $L(1 + 1/N)$ (i.e. patterns of a two-unit system with $L = 1$ can correspond to a four-unit system with $L = 2$).

Actually, with increasing N the variety of possible regular solutions, classified by their symmetry, becomes larger. Thus, with $N = 4$ we obtained regular 1:3 pattern that admit symmetry (17) with $M = N/2$ ($V_{sw}/V_{th} = 2.75$, Figure 10a) and 1:5 pattern with $M = N$ ($V_{sw}/V_{th} = 4.5$, Figure 10c).

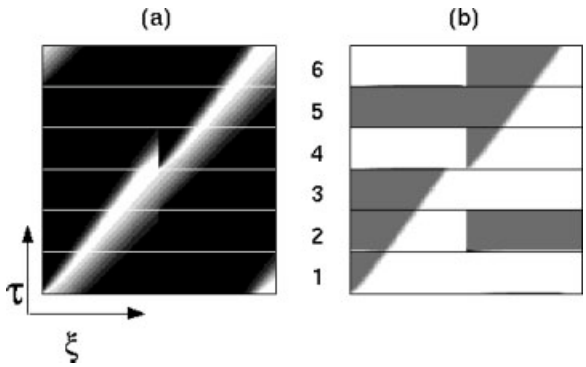

Figure 7. Typical regular 1:3 solution of a two-unit loop reactor showing the temperature (a) and conversion (b) patterns during one oscillation period in a stationary coordinate system (ξ, τ).

Horizontal lines separate switching intervals and are marked by numbers (during the 1st, 3rd, and 5th switching the feed enters unit 1, while during the 2nd, 4th, and 6th—unit 2). $B = 6B_0$, $V_{sw}/V_{th} = 3.0$; other parameters as in Figure 2.

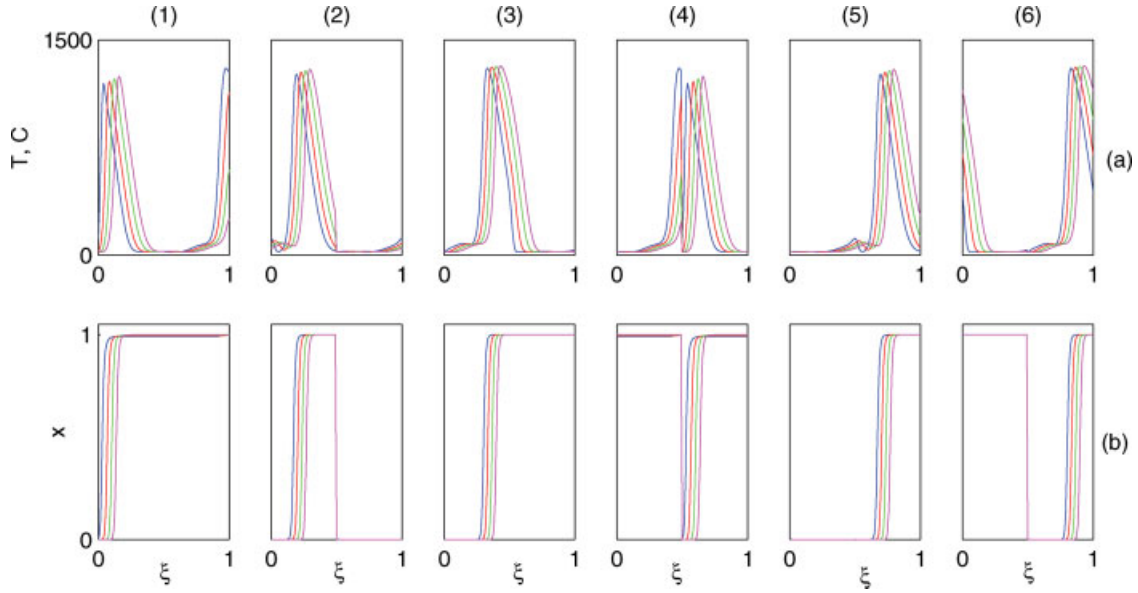

Figure 8. A typical sequence in a two-unit loop reactor of temperature (a) and conversion (b) spatial profiles during one oscillation period of a regular 1:3 solution shown in Figure 7.

Each Plate (1–6) corresponds to the switching interval marked in Figure 7. The parameters as in Figure 7. [Color figure can be viewed in the online issue, which is available at www.interscience.wiley.com.]

Other symmetries with $M \neq N$ can be also expected. (Altimari et al.[24] in a recent study of a three-unit system detected multiple regular solutions that do not obey Eq. 17 or, formally, it can be applied with $M = 1$). Moreover, the structure of subdomains within each finger becomes more complicated with increasing N: With $N = 2$ regular 1:n patterns are found for most of the "finger" domain, while with $N = 4$ subdomains of quasi-periodic and even chaotic behavior are found next to the boundaries (compare regular and quasiperiodic 1:3 patterns shown in Figure 7 with $N = 2$ and in Figure 10b with $N = 4$, simulated under the same conditions).

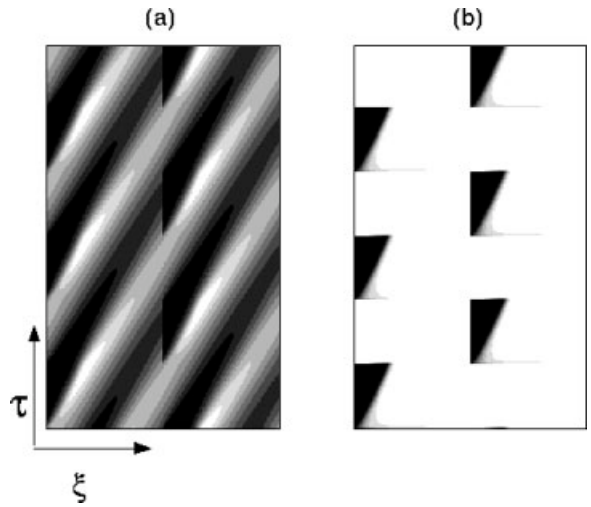

Figure 9. Typical regular $(1:3)_3$ solution of a two-unit loop reactor showing the temperature (a) and conversion (b) patterns during one pulse rotation period in a stationary coordinate system (ξ, τ).

$B = 8B_0$, $v = 1$, $V_{sw}/V_{th} = 3.0$; other parameters as in Figure 2.

The detailed study of all possible solutions is beyond the present study as we are interested mainly in portraying the QNFP boundary. Several scenarios of patterns transformation to chaos within a continuous domain of switching velocities are portrayed by Russo et al.[23] and Altimari et al.[24]

Maximal Temperature Rise and Conversion. The highest maximal temperature is achieved within the QFP domain around $V_{sw} = V_{th}$ (Figure 11a). Within each QNFP domain the maximal temperature rise (at fixed B) is obtained around its lower-switching boundary and T_m significantly declines at larger V_{sw}. The time averaged exit conversion is practically unity over most part of the QNFP subdomains (Figure 11b) and declines sharply at the right boundary of each finger. Surprisingly, for these even N-unit systems ($N = 2, 4$) patterns with even n exhibit smaller conversion than patterns with odd n. This may not hold for odd N.

To conclude, we note that while the non-frozen patterns are more complex in nature than the frozen ones they may provide the desired conversion over a wide domain of switching velocities.

Comparison of the finite-unit and asymptotic models

The asymptotic model (6 and 7) was shown to yield reasonable predictions of quasi-frozen solutions of the finite-unit model and the accuracy improves as $N \to \infty$. Elsewhere[31] we derived an approximate design procedure for the FP which can be easily extended to the case of finite N. This analogy between the asymptotic and constant N solutions cannot be extended to the non-frozen patterns. Yet, NFP are viable solutions with good conversion (Figure 11) but they will require intricate control for operation.

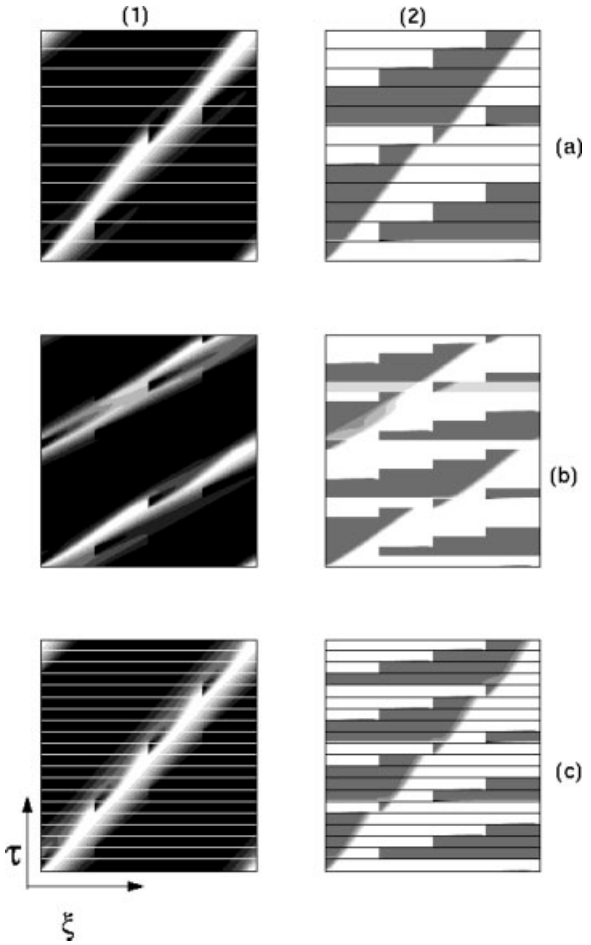

Figure 10. Typical temperature (1) and concentration (2) patterns of the four-unit model showing a regular 1:3 solution (V_{sw}/V_{th} = 2.75, a, obeys symmetry (17) with $M = N/2 = 2$), a quasi-periodic 1:3 solution (V_{sw}/V_{th} =3.0, b) and a regular 1:5 solution (V_{sw}/V_{th} = 4.5, c, obeys symmetry (17) with $M = N = 4$).

Horizontal lines in (a,c) separate switching intervals, $B = 6B_0$,$V_{sw}/V_{th} = 3.0$; other parameters as in Figure 2.

The asymptotic model predicts a continuous NFP domain with $V_{sw} > V_{sw}^{mx}$ with wide subdomains of regular 1:n solutions (we traced them up to $n = 3$) separated by gaps of complex and quasi-periodic behavior. Other subdomains probably can be detected outside the set of parameters considered in the present article (yet, with larger B).

Simulations conducted with a finite-unit model for small N also revealed clearly distinguished finger-shaped domains of regular 1:n locked solutions separated by gaps in which the solution is either extinguished at low B, or chaotic at large B. However, their boundaries as well as the pattern features cannot be predicted by the continuous model. This is probably due to the small N used in simulations. Another reason is that the applied BC (8) imposed in the asymptotic model by matching of the inlet and outlet temperature are reasonable for simple "frozen" solutions and are not valid for the general case. Anyway, to predict the finite-unit system behavior with small N we need to conduct its direct numerical simulations.

The NFP domain with $V_{sw} < V_{sw}^{mn}$ (to the left of the FP domain) predicted by the asymptotic model was not detected using the finite-unit model. Nevertheless, the obtained results can be useful for the following analysis: In the case of no external forcing ($V_{sw} = 0$) model (6–8) corresponds to the limiting circular loop reactor model. Thus, detection of the left nonfrozen patterns domain allows to get some insight into the operation condition domain of the CLRs.

Comparison of Different Reactor Types

In comparison the various approaches we focus on the following features; robustness, conversion and construction.

Robustness

Of the many fingers of the LR solutions the FP domain provides solutions at the lowest B values. Thus, the LR has a narrow domain of operation of switching velocities, and the domain becomes narrower as the system is less exothermic or the feed flow rate is higher (Figure 2). While this is a drawback, the switching velocity can be set at a value of $1/Le$ for the QFP and at $n/$Le for QNFP, to provide the widest domain of operating conditions. If this condition is achieved the LR operating domain is as large as that of the RFR. This may be intricate when Le is not known exactly. In that case the LR can be very easily controlled. A simple control for QFP, suggested by Barresi et al.[14], is to switch the feed port whenever the temperature in a certain probing position in the next unit, following the feed, reaches a critical value. This was experimentally implemented by us[22] and found to be robust. Theoretically, it can be shown that a

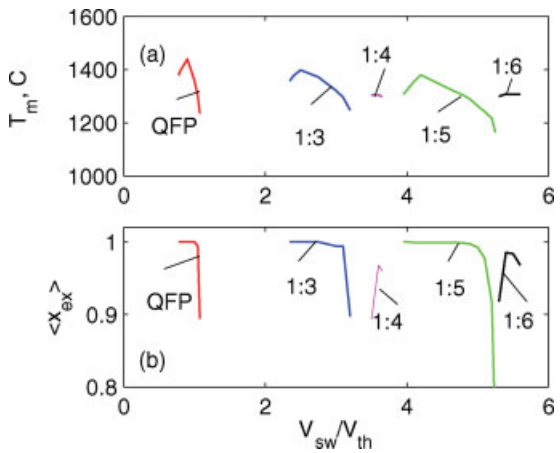

Figure 11. Typical bifurcation map of the two-unit loop reactor model with varying switching velocity V_{sw} showing the maximal temperature T_m (a) and the average exit conversion <x_{ex}> (b).

Numbers mark the type of frequency locked solution, dots mark extinction points. $\nu = 1$, $B/B_0 = 6$, other parameters as in Figure 2. [Color figure can be viewed in the online issue, which is available at www.interscience.wiley.com.]

proper choice of set points and set positions will provide the widest domain. The LR admits a quasi-frozen rotating pattern which is easy to control.

The CLR does not require switching and valves but its solution is time- and space-dependent and difficult to control. Yet, for sufficiently long L and good heat transfer coefficient it can be compared with the LR. The RFR has a wide domain of switching velocities over which it can be maintained.

Comparison of the LR with $V_{sw} = V_{th}$ (i.e. conditions that will establish the maximal temperature) and the RFR or the CLR can be conducted by estimation of the maximal temperature (T_m) using both direct numerical simulations and approximate relations. An inspection of Eqs. 12–14 shows that the maximal temperature in the LR (with $V_{sw} = V_{th}$) and the CLR (of a sufficient length) are practically the same, while in the RFR T_m can be significantly smaller. While high T_m by itself is not an objective we can use the approximation to predict the extinction point upon decreasing B, Da.

Conversion

Conversion in the LR, within the operating domain, is always almost complete. Conversion in the CLR is significantly smaller and is time-dependent. In the RFR the unreacted feed is released for a short time after switching. Yet, increasing L can remedy this problem.

Construction

The CLR requires investment in the special heat exchanger unit. The LR and RFR require solenoid valves to direct the streams. The number of such valves is higher in the LR and increases with the number of units. Moreover, some of the valves are located inside the system and should withstand to high temperatures. This problem can be overcome by one-way valves as we show elsewhere.[22]

Acknowledgments

Work supported by the US Israel Binational Scientific Foundation. MS is a member of the Minerva Center of Nonlinear Dynamics. ON is partially supported by the Center for Absorption in Science, Ministry of Immigrant Absorption State of Israel.

Notation

BC = boundary condition
CLR = circular loop reactor
FP = frozen pattern
LR = loop reactor
NFP = non-frozen pattern
QFP = quasi-frozen pattern
QNFP = quasi-non-frozen pattern
RFR = reverse flow reactor
VOC = volatile organic compounds

Literature Cited

1. Matros YuSh. *Unsteady Process in Catalytic Reactor*. Amsterdam: Elsevier, 1985.
2. Eigenberger G, Nieken U. Catalytic combustion with periodical flow reversal. *Chem Eng Sci*. 1988;43:2109–2115.
3. Matros YuSh, Bunimovich GA. Reverse-flow operation in fixed bed catalytic reactors. *Catal Rev Sci Eng*. 1996;38:1–68.
4. Frauhammer J, Eigenberger G, von Hippel L, Arntz D. A new concept for endothermic high-temperature reactions. *Chem Eng Sci*. 1999;54:3661–3670.
5. Kolios G, Frauhammer J, Eigenberger G. Autothermal fixed-bed reactor concepts. *Chem Eng Sci*. 2000;55:5945–5967.
6. Ben-Tullilah M, Alajem E, Gal R, Sheintuch M. Comparing flow-reversal and inner recirculation reactors: experiments and simulations. *AIChE J*. 2003;49:1849–1858.
7. Ruppel W. Eine Mathematische Beschreibung Wandernder Brennzonen in Schüttschichten. Ph.D. Thesis, Universität Stuttgart, 1980.
8. Berezowski M, Grabski A. Analytical relationship determining the oscillation period of heat-integrated homogeneous tubular chemical reactor without dispersion. *Chem Eng Sci*. 2005;60:1787–1792.
9. Lauschke G, Gilles ED. Circulation reaction zones in a packed-bed loop reactors. *Chem Eng Sci*. 1994;49:5359–5375.
10. Hua X, Mangold M, Kienle A, Gilles ED. State profile estimation of an autothermal periodic fixed-bed reactor. *Chem Eng Sci*. 1998;53:47–58.
11. Matros YuSh. *Catalytic Process Under Unsteady-State Conditions*. Amsterdam: Elsevier, 1989.
12. Haynes TN, Caram HS. The simulated moving bed chemical reactor. *Chem Eng Sci*. 1994;49:5465–5472.
13. Brinkmann M, Barresi AA, Vanni M, Baldi G. Unsteady state treatment of very lean waste gases in a network of catalytic burners. *Catal Today*. 1999;47:263–277.
14. Barresi AA, Vanni M, Brinkmann M, Baldi G. Control of an autothermal network of nonstationary catalytic reactors. *AIChE J*. 1999;45:1597–1602.
15. Fissore D, Barresi AA. Comparison between the reverse-flow reactor and a network of reactors for the oxidation of lean VOC mixtures. *Chem Eng Technol*. 2002;25:421–426.
16. Velardi S, Barresi AA. Methanol synthesis in a forced unsteady-state reactor network. *Chem Eng Sci*. 2002;57:2995–3004.
17. Velardi S, Barresi AA, Manca D, Fissore D. Complex dynamic behavior of methanol synthesis in the ring reactor network. *Chem Eng J*. 2004;99:117–123.
18. Fissore D, Penciu OM, Barresi AA. SCR of NOx in loop reactors: asymptotic model and bifurcation analysis. *Chem Eng J*. 2006;122:175–182.
19. Fissore D, Garan Tejedor D, Barresi AA. Experimental investigation of the SCR of NOx in a simulated moving bed reactor. *AIChE J*. 2006;52:3146–3154.
20. Sheintuch M, Nekhamkina O. The asymptotes of loop reactors. *AIChE J*. 2005;51:224–234.
21. Sheintuch M, Nekhamkina O. Comparison of flow-reversal, internal-recirculation and loop reactors. *Chem Eng Sci*. 2004;59:4065–4072.
22. Madai AY, Sheintuch M. Demonstration of Loop Reactor Operation. *AIChE J*. Submitted.
23. Russo L, Altimari P, Mancusi E, Maffettone PL, Crescitelli S. Complex dynamics and spatiotemporal patterns in a network of three distributed chemical reactors with periodical feed switching. *Chaos Solitons Fractals*. 2006;3:682–706.
24. Altimari P, Maffetone PL, Crescitelli S, Russo L, Mancusi E. Nonlinear dynamics of a VOC combustion loop reactor. *AIChE J*. 2006;52:2812–2823.
25. Barto M, Sheintuch M. Excitable waves and spatiotemporal patterns in a fixed-bed reactor. *AIChE J*. 1994;40:120–130.
26. Sheintuch M, Nekhamkina O. Pattern formation in homogeneous reactor models. *AIChE J*. 1999;45:398–409.
27. Digilov R, Nekhamkina O, Sheintuch M. Catalytic spatiotemporal thermal patterns during CO oxidation on cylindrical surfaces: experiments and simulations. *J Chem Phys*. 2006;124:034709.
28. Wicke E, Vortmeyer D. 1959. Zündzonen heterogener Reaktionen in gasdurchströmten Körnerschichten. *Ber Bunsen-Ges*. 1959;63:145–152.
29. Kiselev OV. *Theoretical Study of the Phenomena of Heat Waves Movement in Catalytic Bed, (in Russian)*. Novosibirsk: Russian Academy of Sciences, Institute of Catalysis, 1993.
30. Frank-Kamenetski DA. *Diffusion and Heat Exchange in Chemical Kinetics*. New York: Princeton University Press, 1955.
31. Nekhamkina O, Sheintuch M. Approximate design of loop reactors. *Chem Eng Sci*. 2008. In press.

Appendix

Circular loop reactor model

The CLR[11] is composed of a one-port loop-shaped tubular fixed-bed reactor with a co-current heat exchanger that couples the inlet and outlet sections. Its mass balance can be described by Eq. 3, while the enthalpy balance can be modeled as a three-zone unit differing in the existence or absence of an external heat exchange:

$$Le\frac{\partial y}{\partial \tau}+v\frac{\partial y}{\partial \xi}-\frac{1}{Pe_{\mathrm{y}}}\frac{\partial^2 y}{\partial \xi^2}=B(1-x)f(y)-S_{\mathrm{T}} \qquad \text{(A1)}$$

with imposed Dankwerts' BC (4). The additional with respect to Eq. 2 source term S_{T} is of a step-wise form:

$$S_{\mathrm{T}}=\begin{cases}\alpha[y(\xi)-y(L-\Delta+\xi)] & \text{if } \xi\in[0,\Delta),\\ 0 & \text{if } \xi\in[\Delta,L-\Delta],\\ \alpha[y(\xi)-y(\xi-L+\Delta)] & \text{if } \xi\in(L-\Delta,L]\end{cases} \qquad \text{(A2)}$$

where α is the dimensionless heat transfer coefficient and Δ is the length of the external heat exchange sections. In order to illustrate the similarity between the CLR and LR schemes it is useful to consider a limiting CLR model with a narrow heat exchange regions ($\Delta \ll L$) and a finite product $\alpha\Delta = O(1)$. Consider the heat balances over the external sections assuming that they are at quasi-steady state with constant temperatures over each section and that the reaction rate is negligible. With account for BC we obtain:

$$v[y|_0-y^{\mathrm{in}}]=\left(\frac{1}{Pe_{\mathrm{y}}}-\frac{1}{Pe_{\mathrm{fy}}}\right)\left(\frac{\partial y}{\partial \xi}\right)_0+\alpha\Delta[y|_L-y|_0] \qquad \text{(A3)}$$

$$0=\left(\frac{1}{Pe_{\mathrm{fy}}}-\frac{1}{Pe_{\mathrm{y}}}\right)\left(\frac{\partial y}{\partial \xi}\right)_{\mathrm{L}}-\alpha\Delta[y|_{\mathrm{L}}-y|_0] \qquad \text{(A4)}$$

where Pe_{fy} is Peclet number defined via the fluid conductivity $[(\rho c_{\mathrm{p}})_{\mathrm{f}} z_0 u_0/k_{\mathrm{f}}]$ and $Pe_{\mathrm{fy}}{}^{-1}$ can be neglected in comparison with $Pe_{\mathrm{y}}{}^{-1}$. Summarizing Eqs. A3 and A4 we obtain:

$$\frac{1}{Pe_{\mathrm{y}}}\left[\left(\frac{\partial y}{\partial \xi}\right)_0-\left(\frac{\partial y}{\partial \xi}\right)_{\mathrm{L}}\right]=v[y(0)-y^{\mathrm{in}}]$$

which coincides with the first of boundary conditions (8). In the limit case $\alpha\Delta\to\infty$ condition (A4) is reduced to $y(0) = y(L)$ yielding the second BC (8). Thus, the limiting CLR model ($\alpha\to\infty$, $\Delta\to 0$) coincides with the asymptotic LR model with $V_{\mathrm{sw}} = 0$.

Manuscript received Jun. 4, 2007, and revision received Jan. 20, 2008.